J Mater Sci: Mater Electron (2020) 31:22926–22932

Mechanical properties and microstructural evolution of solder alloys fabricated using laser-assisted bonding

Hong-Sub Joo[1,2], Choong-Jae Lee[1], Kyung Deuk Min[1], Byeong-Uk Hwang[1], and Seung-Boo Jung[1,*]

[1] *School of Advanced Materials Science & Engineering, Sungkyunkwan University, 2066 Seobu-ro, Jangan-gu, Suwon 16419, Republic of Korea*

[2] *Test & System Package, SAMSUNG Electronics, 158 Baebang-ro, Baebang-eup, Asan-si 32489, Republic of Korea*

Received: 7 July 2020
Accepted: 3 November 2020
Published online: 15 November 2020

© Springer Science+Business Media, LLC, part of Springer Nature 2020

ABSTRACT

The mass reflow (MR) process is widely used in electronic packaging interconnection. However, the conventional MR process can cause thermal damage to components and requires a long process time. The laser-assisted bonding (LAB) process is considered as an alternative soldering process for overcoming these limitations due to its extremely fast process time and high thermal selectivity. The LAB process causes low thermal damage; hence, it can be used to fabricate flexible and stretchable applications. This study investigates the mechanical properties, microstructural variation, and intermetallic reaction between the SAC 305 solder and Cu electrodes. The mechanical properties are investigated using shear tests, while the microstructure is analyzed using scanning electron microscopy and X-ray scans. Furthermore, the reliability of the LAB- and MR-produced SAC 305 solders is assessed using a high-temperature storage test. As a result, the intermetallic compound layer is found to be considerably thinner, and the volume of voids in the solder matrix is lower in the LAB-produced solder than that in the MR-produced solder. The mechanical properties of the LAB-produced solders are enhanced by these microstructural advantages.

1 Introduction

The excellent performance of electronic packaging has led to the miniaturization of numerous components [1, 2]. The importance of interconnection components has increased due to such miniaturization trends because various problems, such as the electromigration phenomena, electrochemical behaviors, warpage problems, and thermal emission issues, occur in these components [3–6]. Different types of interconnection techniques, including soldering, sintering bonding, and transient liquid phase bonding, have been investigated [7–9]. Soldering is considered as a representative interconnection process for providing mechanical, electrical, and thermal connection in electronic packaging. Sn–3.0Ag–0.5Cu (SAC 305)

Address correspondence to E-mail: sbjung@skku.edu

https://doi.org/10.1007/s10854-020-04819-0

alloy systems have been optimized as solder alloys due to their excellent reliability in electronic packaging [10]. However, the soldering processes of SAC 305 have been predominantly performed using the mass reflow (MR) process, which requires a high process temperature and a long process time, because the melting temperature of SAC 305 is 217 °C, which can impair the polymers in devices.

Studies have considered the use of a low-melting temperature solder to reduce thermal damage during the MR process [11, 12]. The use of composite materials or other adhesive materials as replacements for traditional soldering has also been investigated [13]. However, several studies have reported that substitute materials exhibit inadequate reliability for addressing electronic packaging requirements, such as dispersion problems and long-term reliabilities. An advanced soldering process has been suggested to overcome the drawbacks associated with SAC solder usage. Laser-assisted bonding (LAB), which is a highly selective soldering process with an extremely short process time, is considered as an alternative soldering process to MR [14–16]. The LAB process yields finer grains and thinner intermetallic compounds (IMCs) due to the short melting time and is characterized by an excellent manufacturing efficiency. The non-contact properties and the selectivity of this process can decrease the thermal and mechanical damage to components [17]. Accordingly, a flexible and stretchable electronic packaging can be realized using the LAB process due to its remarkable advantages.

The effect of the soldering processes (i.e., LAB and MR processes) on the mechanical property variation and the microstructural evolution during thermal aging is investigated herein. The mechanical properties of the SAC 305 solder are evaluated using the ball shear test. Furthermore, a high-temperature storage test is conducted to assess the effect of the intermetallic compound formation and growth, void shape variation, and grain morphology on the storage time. Moreover, the effect of the microstructures on the mechanical properties is discussed.

2 Experimental procedure

Two types of test kit (Fig. 1) were designed to evaluate the effect of the soldering process on the mechanical properties and the microstructural evolution of the SAC solders. First, a printed circuit board (PCB) for the ball shear test was used. The PCB comprised an electrode with a 230 μm Cu opening in accordance with the ball shear test standard (JESD22-B117A) [18]. In the other case, the test kit comprised a Si chip mounted on a PCB structure. The PCB consisted of a square electrode with 3 mm × 3 mm opening. Furthermore, Si chips with 3 mm × 3 mm × 0.2 mm dimensions and a sputtered Cu electrode were used for mounting.

For the test kit fabrication, the SAC 305 solder paste (S3X58-KVH, KOKI, Japan) was printed on an organic solderability preservative surface-finished PCB. Two types of soldering process were used to evaluate the mechanical properties and the microstructural variation of the material. The MR process was performed using a reflow machine (1809EXL; Heller, USA) at a peak temperature of 270 °C for 5 min. Meanwhile, the LAB soldering process was conducted in two steps (i.e., 60 W for 1 s and 72 W for 1 s) with a 980 nm wavelength laser using a laser bonding machine. The laser irradiation process was divided into two steps, that is pre-heating and soldering processes, to achieve an effective soldering process. The laser irradiation area measured 12 × 12 mm^2 square to cover all solder paste in the test kit.

A high-temperature storage test was performed to evaluate the microstructural variation, mechanical properties, void distribution, and IMC reaction between the solder and Cu. This test was performed for up to 1000 h at 150 °C in an isothermal oven.

The shear tests were conducted using a global bond tester (Dage-4000, Richardson Electronics, Ltd.) in accordance with JEDEC standards (JESD22-B117A). A shear speed of 200 μm/s and a shear height of 30 μm were employed. The cross-sectional microstructure and the fracture mode were evaluated after the shear test using field-emission scanning electron microscopy (FE-SEM; SU-8010; Hitachi, Japan). Moreover, the void shape and ratio of the solder matrix were evaluated using an X-ray scanner (XSCAN-H130, Xavis, Republic of Korea).

3 Results and discussion

Figure 2 depicts the cross-sectional microstructure of the SAC 305 solder joints obtained using the MR and LAB processes. The dependence of the grain size and the IMC layer thickness variation on the high-

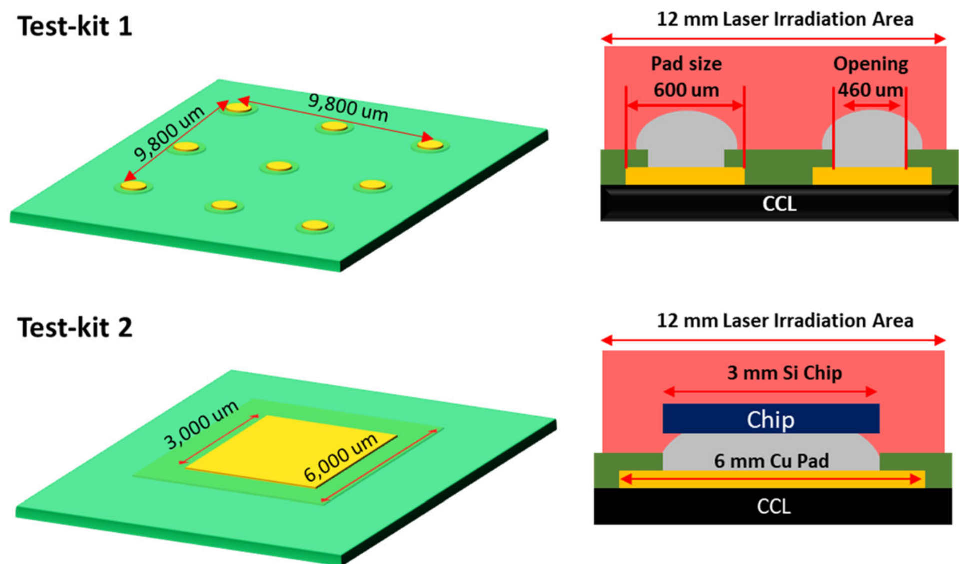

Fig. 1 Schematic of the test kit for evaluating the mechanical properties, microstructure, and void ratio of the SAC 305 solder joints obtained using the MR and LAB soldering processes

temperature storage test time was evaluated from the FESEM micrographs. Each soldering process yielded a Cu_6Sn_5 IMC layer of the as-soldered material [19, 20]. However, the LAB process produced a considerably thinner IMC layer compared to the MR process. Similarly, the LAB process yielded a smaller grain size of the solder matrix compared to the MR process. In both processes, the grain size of the matrix and the IMC layer thickness increased with the thermal aging time. For a given aging time, the IMC thickness associated with the LAB process was always thinner than that produced using the MR process (Fig. 2). Two types of IMC layer were formed at the interface, that is, Cu_6Sn_5 and Cu_3Sn [21, 22]. Cu_6Sn_5 was first formed and grew between SAC 305 and Cu electrode. The preferential growth of the Cu_6Sn_5 IMC layers was then followed by the formation and growth of the Cu_3Sn layer. The thickness of both IMC layers increased with the thermal aging test time. The thickness increase of the IMC layer after the Cu_6Sn_5 growth was saturated was attributed to the increase in the Cu_3Sn layer. The Cu_3Sn layer fabricated through the LAB process was thinner than that fabricated through the MR process. Furthermore, the imbalances between Sn and Cu led to the formation of small voids referred to as Kirkendall voids during the IMC layer growth [23, 24]. The grown grains, IMC

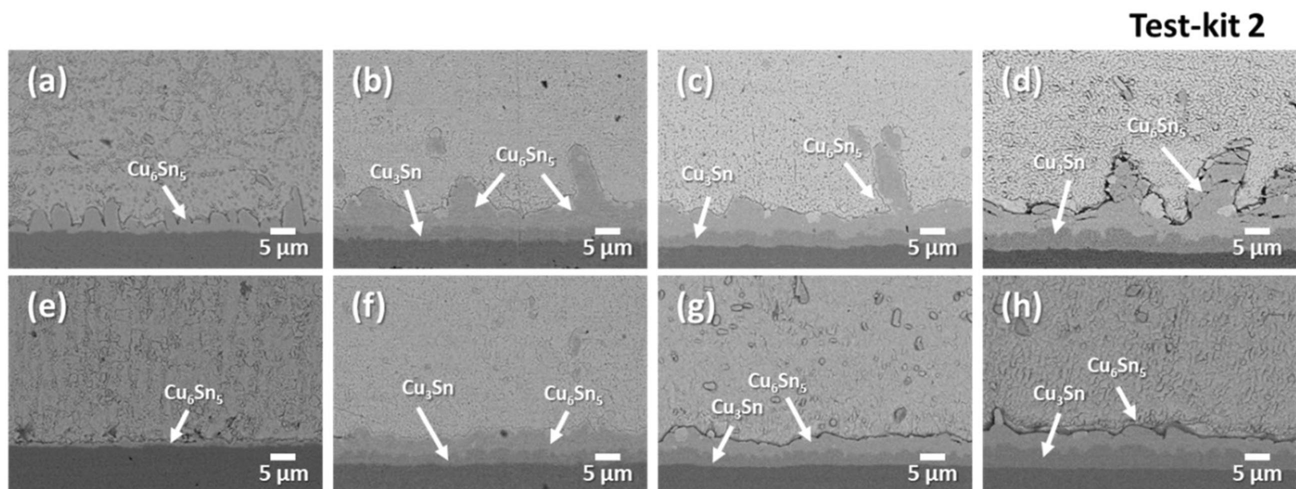

Fig. 2 Cross-sectional microstructure of the solder matrix obtained using the (**a**–**d**) MR and (**e**–**h**) LAB soldering processes and dependence on the high-temperature storage test time: (**a**, **e**) 0 h; (**b**, **f**) 300 h; (**c**, **g**) 500 h; and (**d**, **h**) 1000 h

layer, and voids can deteriorate the mechanical properties of the solder joints.

Figure 3 shows the variation in the IMC layer thickness of the SAC 305 solders joints based on the soldering processes. The IMC layer thickness of the as-fabricated solder joints significantly differed between the two processes (i.e., LAB process: 0.38 μm and MR process: 3.38 μm). The layer thickness and the grain size of the solder matrix increased with the increasing high-temperature storage test time due to the atomic diffusion in the solder alloys. For 1000 h of storage test time, the IMC thickness increased from 3.38 to 17.90 μm and 0.38 to 7.86 μm during the MR and LAB processes, respectively. This thickness increase was mainly attributed to the Cu_6Sn_5 layer growth at relatively low aging times. However, the increase in the IMC layer thickness was ascribed to the Cu_3Sn layer growth after the saturation of the Cu_6Sn_5 layer thickness.

The void distribution in the solder interconnection obtained using different soldering processes (Fig. 4) was investigated using an X-ray scanner. Irrespective of the high-temperature storage test time, the voids in the MR-processed solder joints were larger than those in the LAB-processed joints. The 3 mm × 3 mm chip size and the electrode area were sufficient for forming relatively large voids in the MR-processed solder joints. The long MR-processing time can lead to the aggregation of small voids. However, numerous small voids occurred in the LAB-processed solder joints. The short melting times of the LAB-processed solder alloys can decrease the volume of the voids through void aggregation [25]. The void size of the solder joints for both MR and LAB processes increased with the high-temperature storage test time. After the thermal aging test, small voids attributed to the contraction void formation process and metallic atom diffusion were observed in both processes. An examination of the microstructural evolution revealed that Cu_3Sn was formed after the Cu_6Sn_5 formation at the interface between the SAC 305 and Cu electrodes. The Cu atoms diffused with the Cu_6Sn_5 layer during the IMC layer evolution, and small voids were formed in the solder interconnections. The aforementioned processes led to the void distribution.

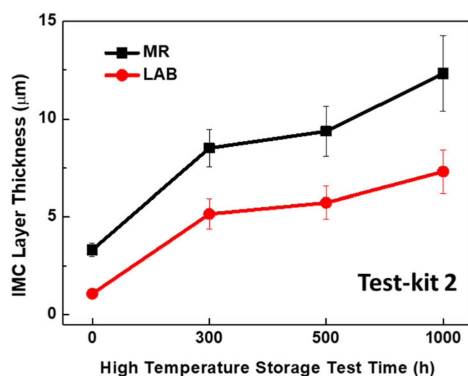

Fig. 3 High-temperature storage test time dependence of the IMC layer thickness variation occurring in the SAC 305 solders obtained using the MR and LAB soldering processes

Figure 5 shows the void ratio of the solder joints depending on the soldering method and the high-temperature storage test time. For all the storage test time conditions, the void ratio associated with the LAB process was considerably lower than that associated with the MR process (i.e., 11.72% and 4.41% for the MR and LAB processes, respectively). The ultra-fast soldering process can induce very rapid phase changes, thereby reducing the void ratio of the solder joints. The void ratio increased with the high-temperature storage test time. Void ratios of ~16.8% and 3.93% were obtained for the SAC solder matrix and the LAB process, respectively, after 1000 h of the storage test. This result is attributed to the contraction and soldering void formation in the solder joints and the atomic diffusion in the solder alloys. The considerably shorter process time of the LAB process compared with that of the MR process resulted in a lower number of voids in the solder joints.

The mechanical properties of the SAC 305 solder joints produced using various soldering processes with thermal aging were investigated using the ball shear test. Figure 6a and b depict the dependence of the solder shear strength and the fracture energy on the thermal aging and the soldering process, respectively. Compared with the MR-generated solder alloy, the LAB-generated alloy exhibited superior mechanical properties under all thermal aging conditions due to the finer grain size of the LAB-processed solder. The short process times of the LAB process can refine the grains in the solder matrix, thereby resulting in the improved mechanical properties of the SAC 305 solder alloys. These improved properties may have resulted from the thinner IMC layer (i.e., compared with the MR process, the LAB process can form a thinner IMC layer at the interface). The void formation in the solder matrix may have also contributed to the superior properties. X-ray

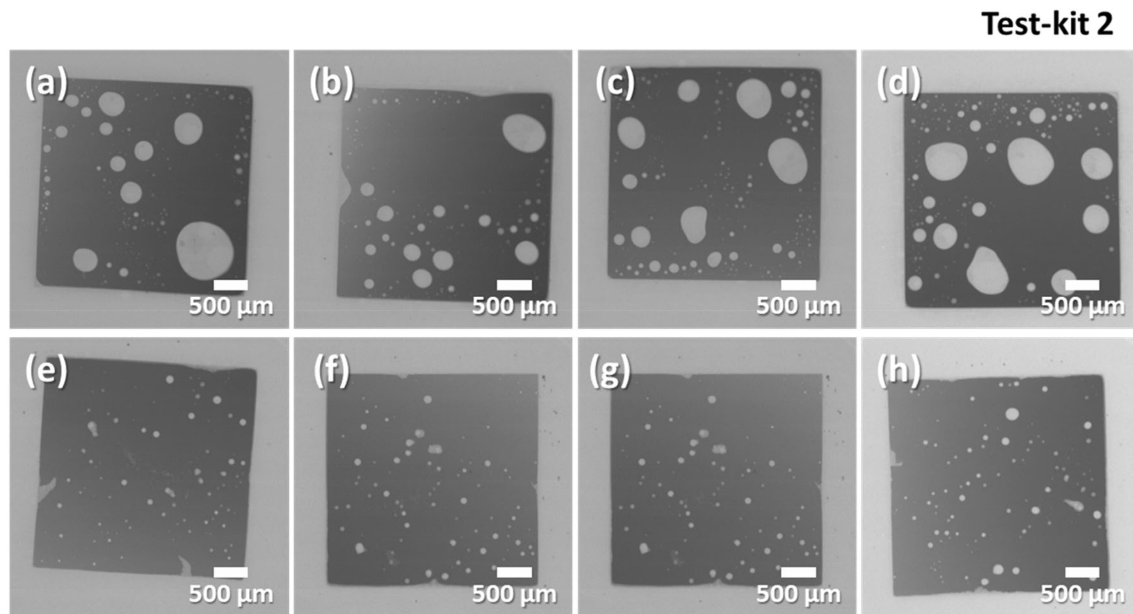

Fig. 4 Void distribution in the solder joints obtained using different soldering processes: (**a**–**d**) MR and (**e**–**h**) LAB. Dependence on the high-temperature storage test time: (**a**, **e**) 0 h; (**b**, **f**) 300 h; (**c**, **g**) 500 h; and (**d**, **h**) 1000 h

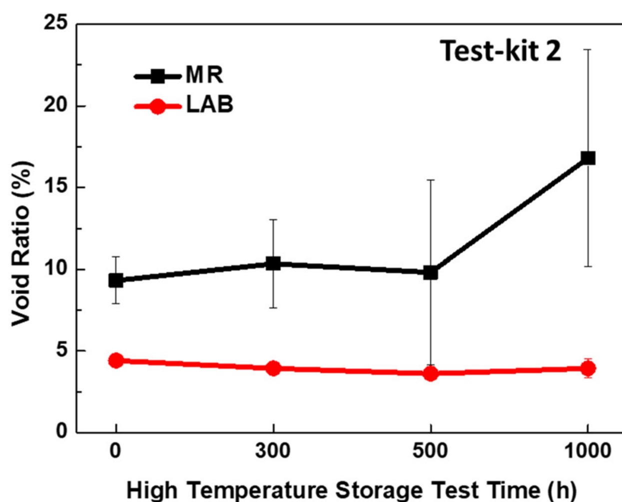

Fig. 5 High-temperature storage test time dependence of the void ratio determined for the SAC 305 solder joints obtained using different soldering processes

scanning revealed that compared with the MR process, the LAB process was characterized by a smaller void ratio and a narrower distribution of small voids. Furthermore, the mechanical reliability of the SAC solder ball fabricated using both processes decreased with the increasing thermal aging time due to the grain and IMC layer growth during the high-temperature storage test. Moreover, the void formation in the solder matrix attributed to voids deteriorated the mechanical properties of the solder alloys. The SAC 305 solder joints with shear strength values of 32.95 and 39.65 MPa and fracture energy values of 1.21 and 1.60 mJ were obtained using the MR and LAB processes, respectively. The results obtained after 1000 h of the high-temperature storage test at 150 °C were similar to those obtained after 0 h.

The fracture mode of the SAC 305 solder joints produced using two types of soldering processes, namely MR and LAB, was investigated using FESEM. Figure 7 shows the fracture surface after shear testing under various thermal aging test conditions and soldering processes. The void distribution and the shapes in the surface significantly differed between the processes, as previously indicated by the X-ray scanning results in Figs 4 and 5. The void formation process was similar to that occurring in the 3 mm × 3 mm Si chip samples, despite the smaller solder ball used in the LAB process. This result suggests that the short process time of the LAB process also affected the mechanical properties and the fracture mode. The solder alloys were characterized by a mixed fracture mode of ductile and brittle fractures. However, the brittle mode became the dominant mode of fracture as the thermal aging test time increased. Dislocations were accumulated in the solder matrix during the shear test, and the shear tip separated the solder joints from the electrode. Therefore, the brittle surface

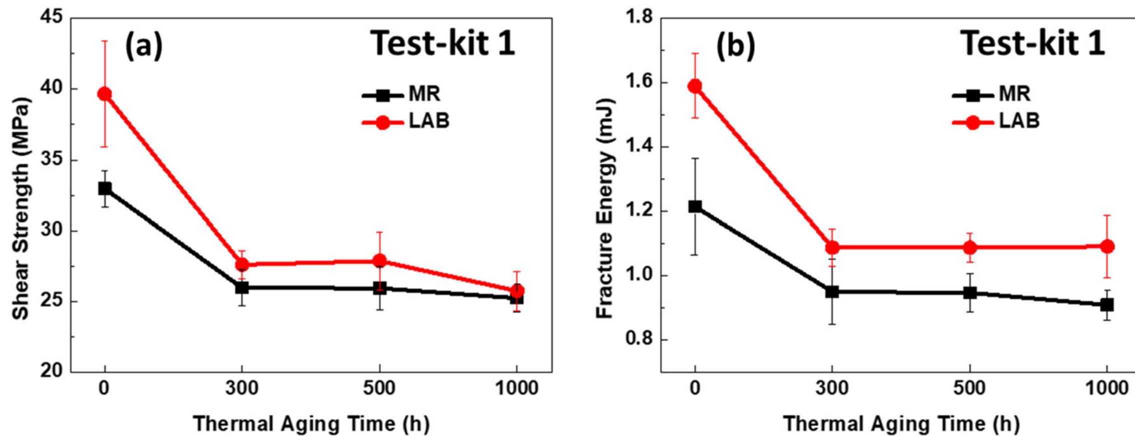

Fig. 6 Temperature storage test time dependence of the **a** shear strength and the **b** fracture energy of the SAC 305 solders obtained using the MR and LAB soldering processes

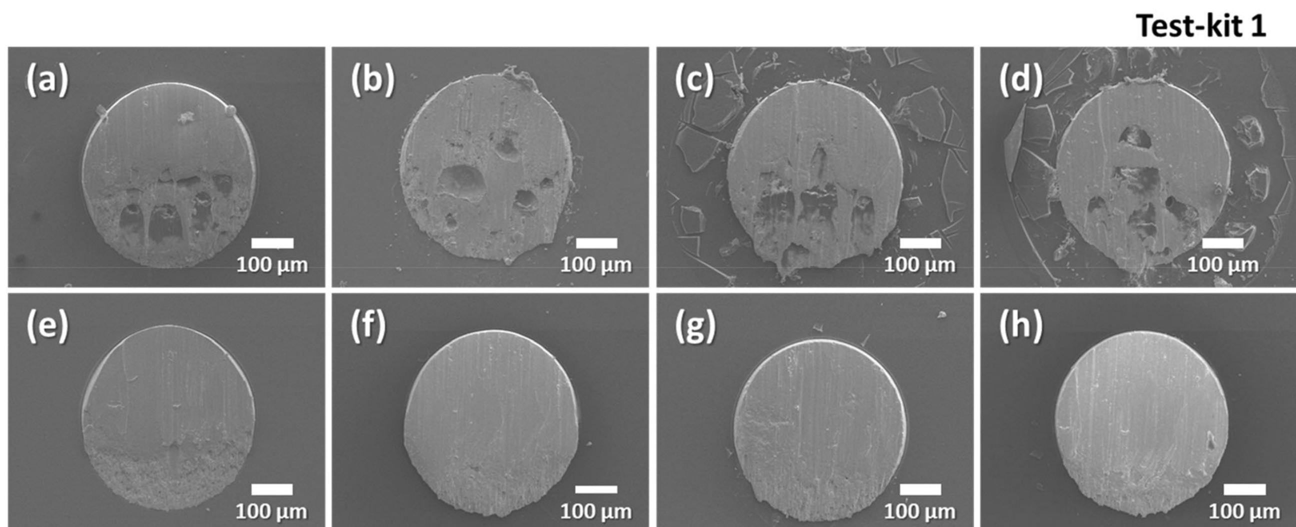

Fig. 7 Fracture surface of the solder alloy after shear tests with different soldering processes: (**a**–**d**) MR and (**e**–**h**) LAB. Dependence on the high-temperature storage test time: (**a**, **e**) 0 h; (**b**, **f**) 300 h; (**c**, **g**) 500 h; and (**d**, **h**) 1000 h

area increased with the thermal aging test time due to the grain and IMC layer growth.

4 Conclusion

In this study, the effects of the soldering process method on the mechanical reliability, void ratio with the Cu electrode, and microstructural evolution of SAC 305 solder alloys were investigated using a high-temperature storage test. The results showed that the mechanical properties of the SAC 305 solder joints obtained using the LAB process were superior to those obtained via the MR process. The short processing time of the LAB process produced solder joints with a finer microstructure and a lower IMC layer thickness compared to those generated using the MR process. Moreover, the void ratio of the LAB-generated solder alloy was considerably smaller than that of the MR-generated alloy. The LAB process showed higher mechanical properties than the MR process as the samples were being fabricated. Furthermore, the mechanical properties of the LAB process exhibited a higher reliability after 1000 h of high-temperature storage test.

Reference

1. M.S. Kim, M.R. Pulugurtha, Y. Kim, G. Park, K. Cho, V. Smet, V. Sundaram, J. Kim, R. Tummala, Microelectron. J. **77**, 66 (2018)
2. Z. Zhu, Y.C. Chan, F. Wu, Microelectron. Reliab. **91**, 179 (2018)
3. R. Tian, C. Hang, Y. Tian, L. Zhao, Mater. Sci. Eng. A **709**, 125 (2018)
4. X. Qi, H. Ma, C. Wang, S. Shang, X. Li, Y. Wang, H. Ma, J. Mater. Sci. Mater. Electron. **30**, 14695 (2019)
5. Y.W. Chang, Y. Cheng, L. Helfen, F. Xu, T. Tian, M. Scheel, M.D. Michiel, C. Chen, K.N. Tu, T. Baumbach, Sci. Rep. **7**, 17950 (2017)
6. H. Zhang, F. Sun, Y. Liu, J. Mater. Sci. Mater. Electron. **30**, 340 (2019)
7. Z. Zhang, C. Chen, Y. Yang, H. Zhang, D. Kim, T. Sugahara, S. Nagao, K. Suganuma, J. Alloys Comp. **780**, 435 (2019)
8. H. Shao, A. Wu, Y. Bao, Y. Zhao, G. Zou, Mater. Sci. Eng. A **680**, 221 (2017)
9. A. Ebrahimian, A.H. Kokabi, Mater. Des. **116**, 599 (2017)
10. M. Wang, C. Qiao, X. Jiang, L. Hao, X. Liu, J. Mater. Sci. Technol. **51**, 40 (2020)
11. Y. Ma, X. Li, W. Zhou, L. Yang, P. Wu, Mater. Des. **113**, 264 (2017)
12. F. Tian, C.F. Li, M. Zhou, Z.Q. Liu, J. Alloys Comp. **740**, 500 (2018)
13. C.J. Lee, K.D. Min, H.J. Park, S.B. Jung, J. Alloys Comp. **820**, 153077 (2020)
14. B. Liu, Y. Tian, W. Liu, W. Wu, C. Wang, Mater. Lett. **163**, 254 (2016)
15. A. Kunwar, S. Shang, P. Råback, Y. Wang, J. Givernaud, J. Chen, H. Mab, X. Song, N. Zhao, Microelectron. Reliab. **80**, 55 (2018)
16. M.S.F. Lima, R. Riva, M.G. Destro, A.M.E. Santo, R.A. Silva Jr., S.M. Guimaraes, Optics Laser Technol. **41**, 159 (2009)
17. A. Kunwar, L. An, J. Liu, S. Shang, P. Råbackd, H. Ma, X. Song, J. Mater. Sci. Technol. **50**, 115 (2020)
18. H. Lee, Y.A. Wang, C.M. Chen, J. Alloys Comp. **765**, 335 (2018)
19. X. Hu, T. Xu, X. Jiang, Y. Li, Y. Liu, Z. Min, Appl. Phys. A **122**, 278 (2016)
20. A.K. Gain, L. Zhang, Materialia **5**, 100234 (2019)
21. K.H. Kim, J. Koike, J.W. Yoon, S. Yoo, J. Electron. Mater. **45**, 6184 (2016)
22. J. Bang, D.Y. Yu, Y.H. Ko, J.H. Son, H. Nishikawa, C.W. Lee, Microelectron. Reliab. **99**, 62 (2019)
23. G. Chen, L. Liu, J. Du, V.V. Silberschmidt, Y.C. Chan, C. Liu, F. Wu, J. Mater. Sci. **51**, 10077 (2016)
24. X. Zhang, X. Hu, X. Jiang, L. Zhou, Q. Li, J. Mater. Sci. Mater. Electron. **31**, 2320 (2020)
25. H. Nishikawa, N. Iwata, J. Mater. Process. Technol. **215**, 6 (2015)

Publisher's Note Springer Nature remains neutral with regard to jurisdictional claims in published maps and institutional affiliations.